

# Dynamic Response of a Water Tower Composed of Interlocked Panels

F. Gurkalo and K. Poutos

**Abstract**—Earthquakes produce some of the most violent loading situations that a structure can be subjected to and if a structure fails under these loads then inevitably human life is put at risk. One of the most common methods by which a structure fails under seismic loading is at the connection of structural elements. The research presented in this paper investigates the interlock systems as a novel method for building structures. The main objective of this experimental study was to determine the dynamic characteristics and the seismic behaviour of the proposed structures compared to conventional structural systems during seismic motions. Results of this study indicate that the interlock mechanism of the panels influences the behaviour of lateral load-resisting systems of the structures during earthquakes, contributing to better structural flexibility and easier maintenance.

**Keywords**—Watertower, earthquake, seismic, interlocked panels

## I. INTRODUCTION

MANY countries around the world experience adverse effects of seismic activity. The importance of water towers is particularly significant in flat areas, where the watertower can be the only source of water to control fire during and after earthquake, as well as to control supplies of drinking water for those inhabiting that area. Thus, the watertowers must remain functional during and after severe ground motions.

Several research groups have looked at fluid-structure interaction and improvement of performance of water tanks [1-4]. There is however less published research into behaviour and performance improvement of the reinforced concrete shafts [5]. During recent earthquakes a number of watertowers collapsed or became non-functional due to damage to the shaft resulting poor ductility in thin reinforced concrete shafts.

This paper presents a new system of assembling shafts for elevated water tanks using panels with a novel interlocked mechanism. This method is based on the use of panels which, readily transported as a flat pack or in pre-formed modules and are quickly assembled on site (Fig. 1).

As a prototype for this study, the geometry of the panels and the interlocked mechanism was designed using the AcerMetric© interlock systems [6].

A full-scale elevated watertower was modelled and analysed using Finite Element analysis software ANSYS 14 Workbench [7]. Reinforced concrete was used as building material for watertower models, and steel for the interlocked mechanisms. The sloshing effect of the water inside the watertank was modelled using fluid-structure interaction system. The analysis was carried out in the frequency domain with a modal analysis procedure according to Eurocode 8 [8].

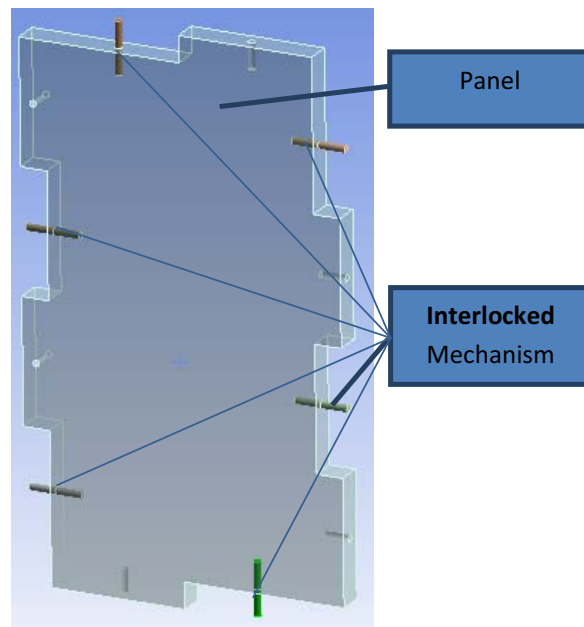


Fig. 1 Proposed interlocked panel model

## III. CASE OF STUDY

In this study three watertowers with same geometric properties and water tanks but different shafts were modelled. Model 1 was modelled as a watertower with a monolith shaft (Fig. 2a). Model 2 and Model 3 were modelled as watertowers composed of interlocked panels (Fig. 2b and 2c respectively). The integrated interlocked mechanism allowed rotation of panels in all directions in Model 2 but restricted any movements and rotations in vertical direction in Model 3. All models had fixed support.

F. Gurkalo is with Department of the Built Environment, Anglia Ruskin University, Chelmsford, CM1 1SQ, UK (filip.gurkalo@anglia.ac.uk).

K. Poutos is with Department of the Built Environment, Anglia Ruskin University, Chelmsford, CM1 1SQ, UK (konstantinos.poutos@anglia.ac.uk).

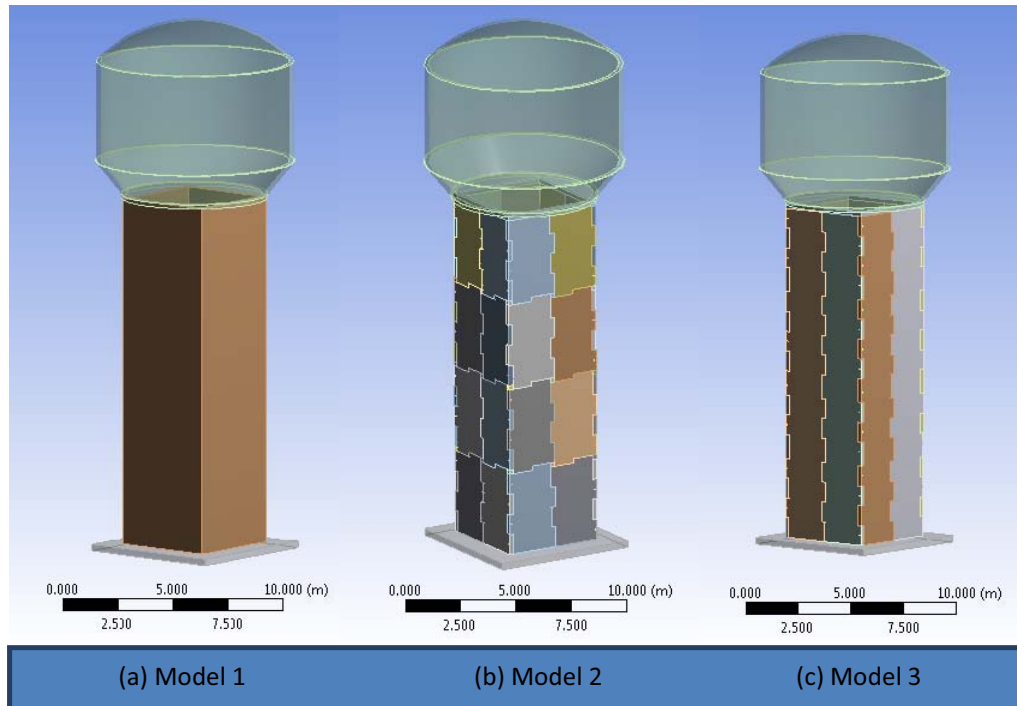


Fig. 2 Three models for analysis (a) Model 1 (b) Model 2 (c) Model 3

Material for panels was assumed as concrete with frictionless contact between panels. The interlocked mechanism was modelled as a bar with 50 mm diameter. Bonded contact between steel bars and the concrete panels was assumed. Connections between interlocked panels are presented in Fig. 3. Specification of the water towers and material properties are provided in Table I and Table II respectively.

TABLE I  
GEOMETRIC PROPERTIES OF THE ANALYSED WATER TANKS

Vessel volume	300 m <sup>3</sup>
Height	7.85 m
Inner diameter	8.6 m
Vessel thickness	0.2 m
Roof thickness	0.12 m
Bottom slab diameter	6.6 m
Bottom slab thickness	0.3 m
Mass of the empty vessel	$1,1526 \cdot 10^5$ kg
Staging outer dimensions	4.4 x 4.4 m
Thickness of a staging	0.2 m
Foundation plate dimensions	6.4 x 6.4 x 0.3 m
Length of a staging	16 m
Mass of the monolith staging (Model 1)	$1.3071 \cdot 10^5$ kg
Mass of the shaft composed of interlocked panels (Model 2)	$1.3148 \cdot 10^5$ kg
Mass of the shaft composed of interlocked panels (Model 3)	$1.3127 \cdot 10^5$ kg
Total mass of model 1	$2.7639 \cdot 10^5$ kg
Total mass of model 2	$2.7716 \cdot 10^5$ kg
Total mass of model 3	$2.7695 \cdot 10^5$ kg

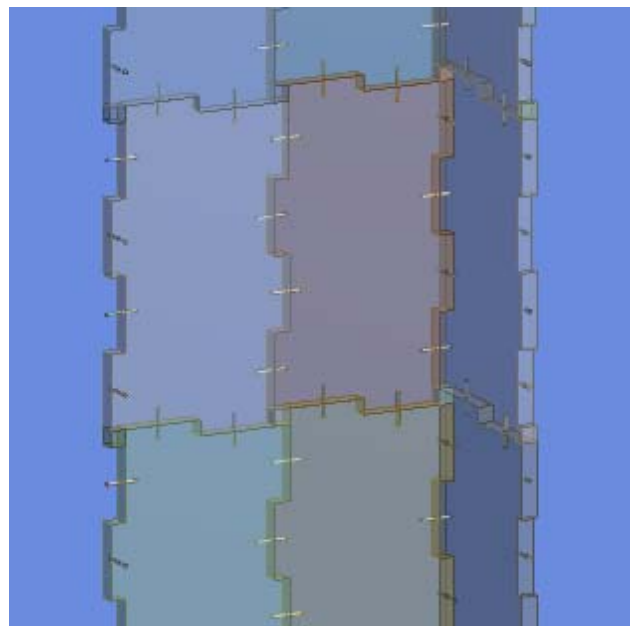


Fig. 3 Middle segment of Model 2 shaft demonstrating close-up of connections between interlocked panels

The watertowers were analysed during two conditions: fullwater tank (300 m<sup>3</sup> water) and empty water tank. Water was modelled using fluid-structure interaction system by two mass model proposed by Hoursner [9].

In this study, modal and after response-spectrum analyses with Square Root of the Sum of the Squares (SRSS) method [10] were employed to determine seismic behaviour of

watertowers. A response spectrum data of Yorba Linda and Norcia-Italy earthquakes with magnitudes 4.26 and 5.9 (Richter scale) respectively were taken from The Pacific Earthquake Engineering Research Centre (PEER) ground motion database [11]. Those magnitudes were chosen to be representative of commonly encountered seismic forces across the world that would have a potential for causing structural damage.

TABLE II  
MATERIAL PROPERTIES

	Concrete	Steel
Density, kg/m <sup>3</sup>	2300	7850
Poisson ratio,	0,18	0,3
Young's Modulus, Pa	$3 \cdot 10^{10}$	$2 \cdot 10^{11}$

#### IV. FLUID-STRUCTURE INTERACTION

A complete dynamic analysis of a structure which contains liquid, such as the water tank, requires the hydrodynamics effect to be considered during the analysis. The hydrodynamics effect can be modelled using different simplified analytical methods such as single lumped-mass model or single degree of freedom (SDOF), two or more masses model, fluid-structure system and finite element model (FEM). Comparison and evaluation of these methods was done by Livaoglu and Dogangun [12]. In this study, a two degree of freedom (2DOF) spring-system of fluid-structure interaction (FSI) was adopted (Fig. 4) from Eurocode 8.

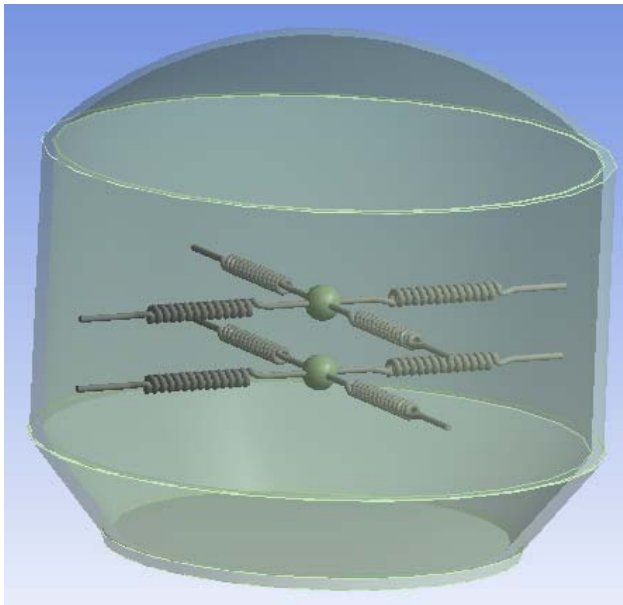


Fig 4 Two degree of freedom spring-system

Parameters of spring-mass model were obtained according to Eurocode 8: an equivalent circular container of same volume and diameter equal to diameter of a tank at top level of liquid was considered.

The height of the equivalent cylinder tank  $H = 5,165 \text{ m}$  and radius  $R = 4,3 \text{ m}$ , so  $\frac{H}{R} = \frac{5,165}{4,3} = 1,2$  and the parameters for the spring-model are represented in the Table III.

Parameters  $h_i$  and  $h_c$  were corrected according to geometric properties of the modelled water tank.

A mass  $m_c$  was connected to the wall of the tank by four springs. Each spring had a total longitudinal stiffness in one direction defined as (1), where  $\omega_{cn}^2$  is sloshing frequency which can be calculated by (2), where  $\lambda_1 = 1,841$  taken from Bessel function of the first order and  $\gamma = H/R$ .

$$K_c = \omega_{c1}^2 m_c \quad (1)$$

$$\omega_{cn} = \sqrt{g \frac{\lambda_n}{R} \tanh(\lambda_n \gamma)} \quad (2)$$

However, in slender tanks the sloshing frequencies become almost independent of  $\gamma$ , thus for tanks with  $\gamma$  larger than 1 Eurocode 8 provides (3).

$$\omega_{c1} = 4,2/\sqrt{R} \quad (3)$$

For the 'full' tank case  $\gamma = 1,2$  so the first sloshing frequency  $\omega_{c1} = 2,0254 \text{ rad/s}$  and the stiffness of springs is

$$K_c = 4,88138 \cdot 10^5 \text{ N/m}.$$

The values of impulsive and convective masses and levels of connection points are represented in Fig. 5 and Table IV.

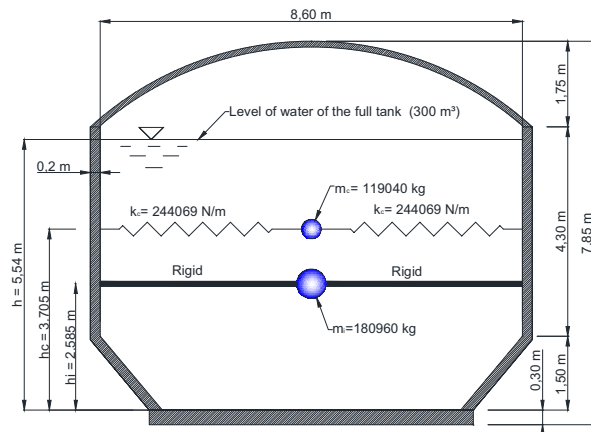


Fig. 5 Modelled water tank

TABLE III  
RECOMMENDED DESIGN VALUES FOR THE FIRST IMPULSIVE AND CONVECTIVE MODES OF VIBRATION AS A FUNCTION OF THE TANK HEIGHT-TO-RADIUS RATIO (H/R) [EC 8]

H/R	C <sub>1</sub>	C <sub>c</sub> (s/m <sup>1/2</sup> )	m <sub>i</sub> /m	m <sub>c</sub> /m	h <sub>i</sub> /H	h <sub>c</sub> /H	h' <sub>i</sub> /H	h' <sub>c</sub> /H
0,3	9.28	2.09	0.176	0.824	0.400	0.521	2.640	3.414
0,5	7.74	1.74	0.300	0.700	0.400	0.543	1.460	1.517
0,7	6.97	1.60	0.414	0.586	0.401	0.571	1.009	1.011
1,0	6.36	1.52	0.548	0.452	0.419	0.616	0.721	0.785
1,2	6.24	1.504	0.6032	0.3968	0.427	0.6456	0.6546	0.7646
1,5	6.06	1.48	0.686	0.314	0.439	0.690	0.555	0.734
2,0	6.21	1.48	0.763	0.237	0.448	0.751	0.500	0.764
2,5	6.56	1.48	0.810	0.190	0.452	0.794	0.480	0.796
3,0	7.03	1.48	0.842	0.158	0.453	0.825	0.472	0.825

TABLE IV  
VALUES OF MASS AND HEIGHT OF IMPULSE AND CONVECTIVE MODES OBTAINED FROM EURO CODE 8

'Full' Tank Case	
Mass of water	$m = 300000 \text{ kg}$
Impulsive mass of water	$m_i = 180960 \text{ kg}$
Convective mass of water	$m_c = 119040 \text{ kg}$
Height from the base of the point of application of the resultant of the impulsive hydrodynamic wall pressure	$h_i = 2.585 \text{ m}$
Height from the base of the point of application of the resultant of the convective hydrodynamic wall pressure	$h_c = 3.705 \text{ m}$
Height from the base of the point of application of the impulse mass for the overturning moment	$h'_i = 3.381 \text{ m}$
Height from the base of the point of application of the convective mass for the overturning moment	$h'_c = 3.949 \text{ m}$

V. MODAL ANALYSIS AND RESPONSE SPECTRUM ANALYSIS

According to Eurocode 8, the sum of the effective modal masses is at least 90% of the total mass of the structure in each direction, so it was required to find 50 first modes of all the models. Block Lanczos algorithm [13] was employed for extracting the modes.

To evaluate the dynamic response of the elevated water tanks, spectral accelerations of earthquakes with magnitudes of 4.29 and 5.9 were applied, as represented in Fig 6.

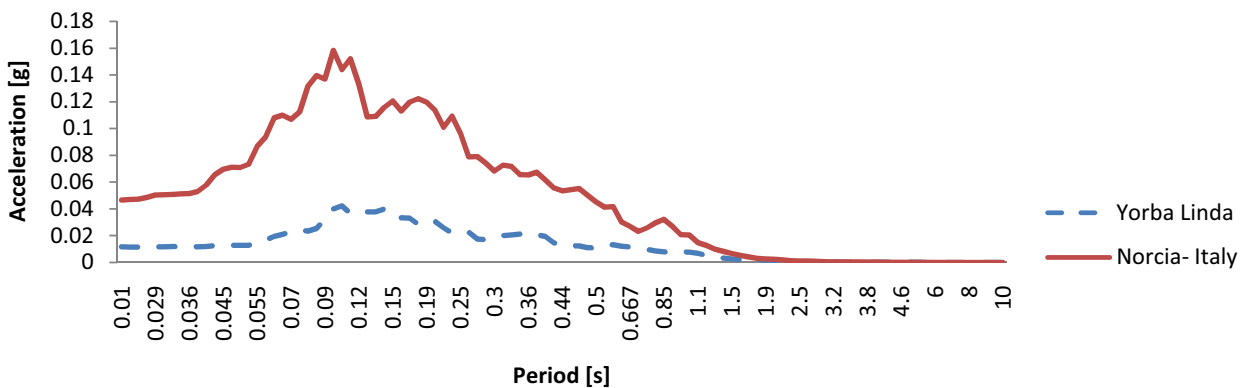


Fig. 6 Spectral acceleration of Yorba Linda and Norcia-Italy horizontal records from PEER

The response spectrum analysis was carried out using 5% viscous damping, as recommended by Eurocode 8.

Progressive schematic Workbench project was prepared for all models under 'full' and 'empty' conditions. Geometry modelling and static analysis were performed using static structural template. After that all results were transferred to modal analysis template and 50 first modes were extracted

Finally, the modal analyses results were transferred to response spectrum template where two spectrum analyses were then conducted using frequency domain data of Yorba Linda and Norcia - Italy earthquakes. The Workbench project for Model 3 under 'full' condition is represented in Fig 7.

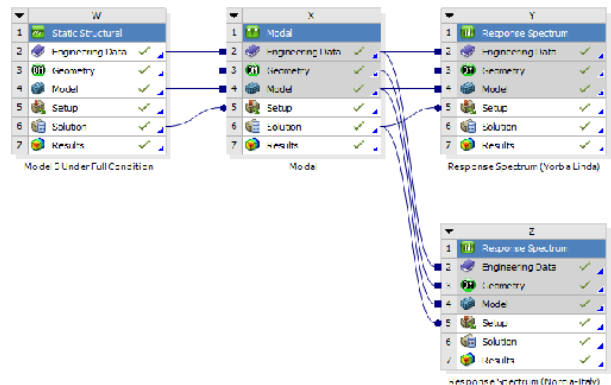


Fig.7 Workbench project schematic of Model 3 under 'full' condition

VI. RESULTS AND DISCUSSION

Tables V and VI represent frequencies of the first 10 modes of the modal analysis under ‘full’ and ‘empty’ conditions respectively. From the modal analysis results it can be observed that the fundamental frequencies of all three models are very similar. However, with incrementally increasing modes, the difference in frequencies between Model 1 and the other two models become more noticeable. This phenomenon may be explained by the fact that Models 2 and 3 are more ductile than Model 1. Fig. 8 and Fig. 9 represent frequencies of all 50 modes under ‘full’ and ‘empty’ conditions respectively. The natural frequencies of Model 2 and Model 3 are similar.

TABLE V  
FREQUENCIES OF THE FIRST 10 MODES FROM MODAL ANALYSIS UNDER FULL CONDITION

Mode	Frequency [Hz]		
	Model 1	Model 2	Model 3
1.	2.6040	2.3558	2.4030
2.	2.6050	2.3566	2.4163
3.	12.983	9.6604	10.388
4.	14.077	12.867	13.025
5.	18.273	15.054	15.420
6.	18.368	15.086	15.841
7.	18.876	15.978	16.784
8.	24.021	20.276	21.604
9.	29.916	22.097	22.250
10.	30.496	22.294	22.775

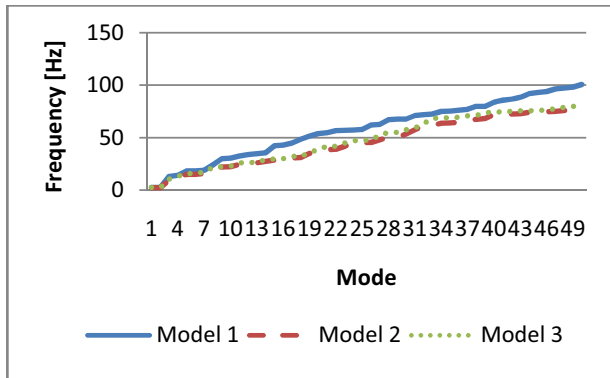


Fig. 8 Frequencies of the first 50 modes under ‘full’ condition

TABLE VI  
FREQUENCIES OF THE FIRST 10 MODES OF MODAL ANALYSIS UNDER ‘EMPTY’ CONDITION

Mode	Frequency [Hz]		
	Model 1	Model 2	Model 3
1.	4.5106	4.0619	4.1567
2.	4.5108	4.0825	4.1810
3.	12.97	9.6334	10.395
4.	18.551	15.263	15.629
5.	18.61	15.659	16.075
6.	18.892	16.216	16.805
7.	24.055	20.463	21.608
8.	26.49	22.591	23.015
9.	30.331	22.865	23.391
10.	30.909	24.31	24.596

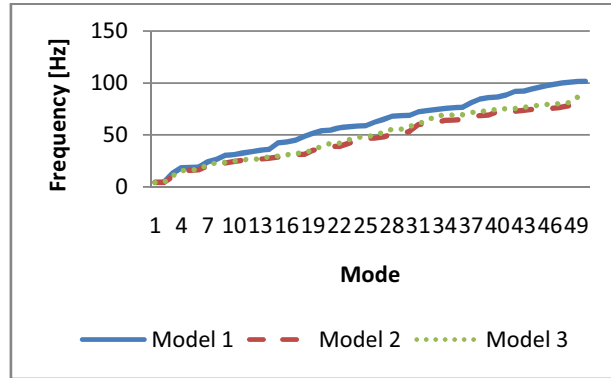


Fig. 9 Frequencies of the first 50 modes under ‘empty’ condition

The deformations of all three models under ‘full’ condition resulted from the response-spectrum analysis using data of Yorba Linda and Norcia-Italy earthquakes are represented in Fig 10. Model 1 and Model 2 show comparable deformation, however the difference in deformation between Model 1 and Model 3 is 13.9% during Yorba Linda earthquake. The higher amplitude earthquake resulted in 17% greater deformation of Model 2 and 2% smaller deformation of Model 3 compared to Model 1. The deformation of Model 1, Model 2 and Model 3 increased by 1.9601 mm, 2.543 mm and 2.0219 mm respectively. It can be observed that deformation of Model 2 and Model 3 increased more rapidly with increasing earthquake amplitude compared to Model 1.

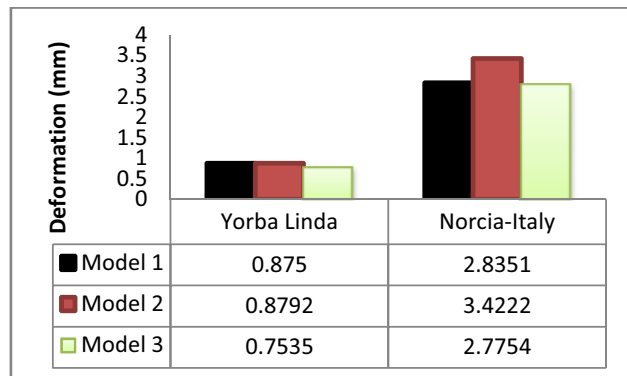


Fig. 10 Maximum directional deformation under ‘full’ condition

The deformations of all three models under ‘empty’ condition derived from the response-spectrum analyses are represented in Fig 11. During the earthquake with amplitude 4.26 the deformation of Model 1 was 19% smaller than deformation of Model 2 and 1% larger than deformation of Model 3. The earthquake with amplitude 5.9 resulted in 28% greater deformation of Model 2 and 18% greater deformation of Model 3 compared to the deformation of Model 1. The deformation of Model 1, Model 2 and Model 3 increased by 1.1476 mm, 1.6624 mm and 1.4868 mm respectively. Similar to the ‘full’ condition, the deformation of Model 2 and Model 3 increased more rapidly with increasing earthquake amplitude compared to Model 1.

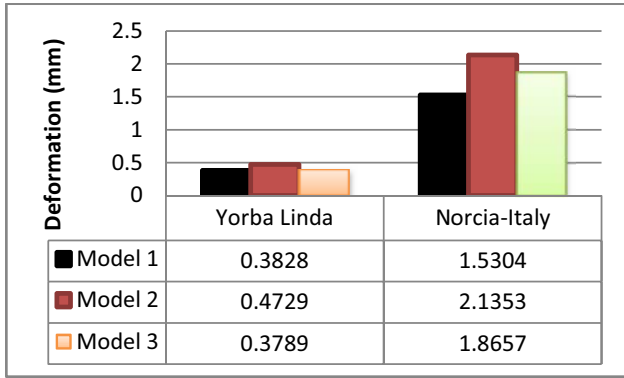


Fig. 11 Maximum directional deformation under 'empty' condition

During Yorba Linda event with magnitude 4.26, the increase in deformation of 'full', compared to 'empty', Model 1, Model 2 and Model 3 increased by 229%, 186% and 199% respectively. During Norcia-Italy event with magnitude 5.9, the deformation of Model 1, Model 2 and Model 3 was greater in 'full' compared to 'empty' condition by 185%, 160% and 149% respectively.

Fig. 12 represents shear stresses of the three models and demonstrates that Model 2 and Model 3 have shear stress distribution different to that of Model 1. In Model 2, every interlocked panel distributes shear forces equally along the shaft and the highest shear stress results within connections between panels. Equivalent (von-Mises [14]) stress distribution in all three models is shown in Fig. 13.

The difference in stress distribution within monolith shaft and shafts composed of the interlocked panels can be appreciated. The panels of Model 2 and Model 3 rely on flexible joints to withstand deformation forces and thus distribute stresses more efficiently along the whole shaft. In contrast, in Model 1 stress is maximum locally next to the support and the deformation results in indirect damage of the monolith staging.

VII. CONCLUSION

A new type of staging that can be used in conceptual design of watertowers is proposed in this paper. Employing the novel method of constructing watertower staging using interlocked panels appears to have several advantages over the conventionally built monolith shafts under seismic conditions.

The flexible joints of the proposed mechanism take on the greatest stress during seismic activity leaving the interlocked concrete panels less susceptible to cracks and damage, compared to the monolith shafts. The new system provides better ductility and lateral stress capacity for the watertower shafts. Moreover, it should allow for the replacement of cracked or damaged panels in a timely manner after earthquakes, avoiding the need to rebuild the whole structure from scratch. Interlocked mechanisms with different stiffness can be used to meet specific requirements of different geographical areas.

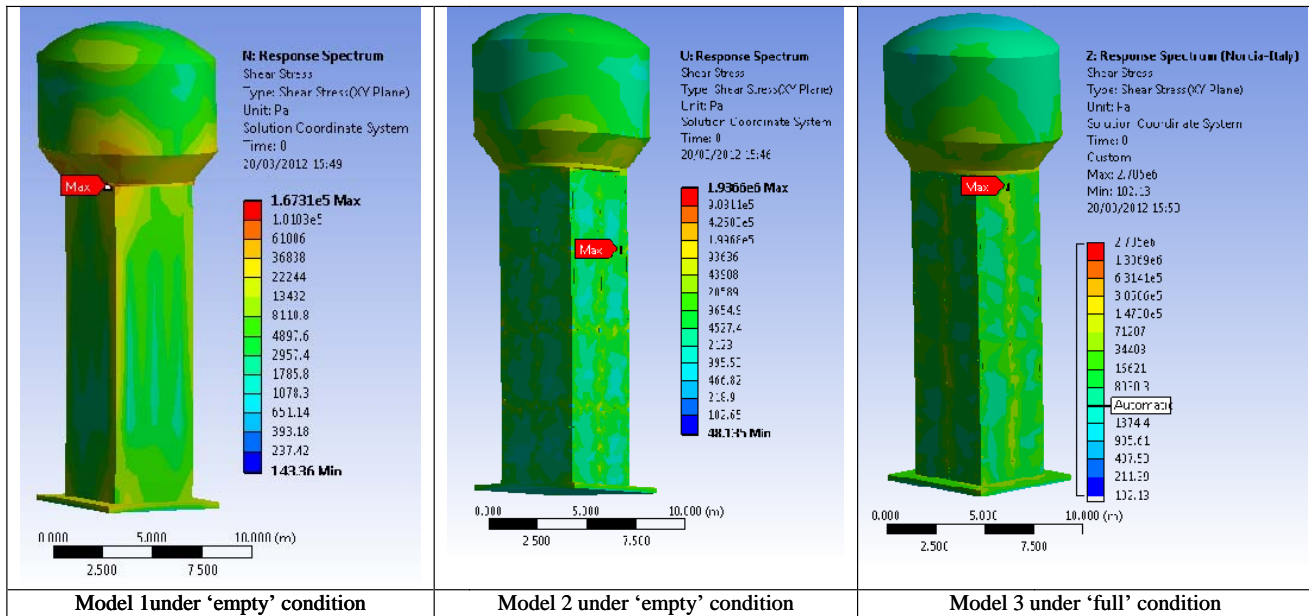


Fig. 12 Shear Stress in XY plane distribution (Pa)

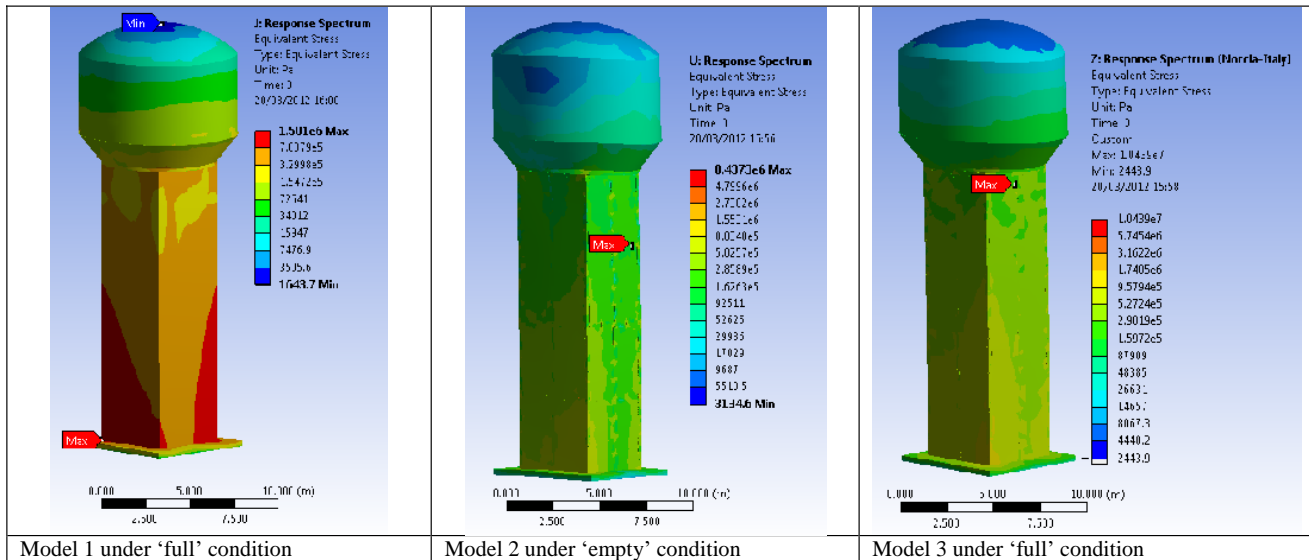


Fig. 13 Von-Mises stress distribution (Pa)

REFERENCES

[1] Algreane, G. A., Osman, S. A., Karim, O. and Kasa, A., 2011. Behavior of Elevated Concrete Water Tank Subjected to Artificial Ground Motion. *EJGE*, 16 (Bund. D), pp.387-406.

[2] Malhotra, P. K., Wenk, T. and Wieland, M., 2000. Simple Procedure for Seismic Analysis of Liquid-Storage Tanks. *Structural Engineering International*, 2/2000, pp. 197-201.

[3] Gareane, A.I., Algreane, G. A., Osman, S. A., Karim, O. and Kasa, A., 2011. Study the Fluid Interaction due to Dynamic Response of Elevated Concrete Water Tank. *Australian Journal of Basic and Applied Science*, 5(9), pp.1084-1087.

[4] El-Rakabawy, M. M., El-Arabaty, H. A. and El-Sherbiny, M. G., 2005. Response of Elevated Water Tanks to Seismic Loads. *ICSGE*, 11<sup>th</sup>

[5] Rai, D. C., 2002. Review of Code design Forces for Shaft Supports of Elevated Water tanks. 12<sup>th</sup> Symposium on Earthquake Engineering, pp.1407-1418.

[6] AcerMetric©. 2010 The AcerMetric© System, www.acermetric.co.uk

[7] ANSYS, INC., 2009. Ansys Workbench user's guide.

[8] Eurocode-8, 2006. Design of structures for earthquake resistance – Part 4: Silos, tank and pipelines. European Committee for Stabilisation, Final PT Draft.

[9] Housner, G.W., 1963. The Dynamic Behaviour of Water Tanks . *Bulletin of Seismological Society of America*, 53(2), pp.381-387.

[10] Jain, S. K. and Jaiswal, O. R., 2005. Modified proposed provisions for aseismic design of liquid storage tanks. *Journal of Structural Engineering*, 32(3,4), pp.195-206, pp.297-310.

[11] Pacific Earthquake Engineering Research Center, 2011. Users Manual for the PEER Ground Motion Database Web Application.

[12] Livaoglu, R. and Dogangun, A., 2006. Simplified seismic analysisprocedures for Elevated tanks considering fluid-structure interaction. *Journal of Fluids and Structures*, 22, pp.421-439.

[13] Gutknecht, M. H. and Loher D., 2009. Block and Band Lanczos Algorithms: a Review of Options, Seminar for Applied Mathematics, ETH Zuri

[14] Von Mises, R.,1913. *Mechanik der festenKörperimplastischdeformablenZustand*. Göttin. Nachr. Math. Phys., vol. 1, pp. 582-59.